**Plishner Radio Astronomy and Space Science Center**

# Ionospheric Reflection Variation During Sunrise and Sunset and Predictions for the 2017 Total Eclipse

Richard Russel

Deep Space Exploration Society

## Abstract

The Plishner Radio Astronomy and Space Science Center is operated by the Deep Space Exploration Society based out of Colorado Springs, Colorado. The Sudden Ionospheric Disturbance (SID) monitor shows significant variations at sunrise and sunset. The Northern Hemisphere will experience a total solar eclipse on August 21, 2017. This paper characterizes the transition characteristics of the SID data and uses this data to predict the effects of the total solar eclipse will have on the SID system signal levels.

## 1.0 Introduction

The sudden ionospheric disturbance (SID) monitor measures the signal strength of a very low frequency (VLF) broadcast station after its signal is reflected off of the ionosphere. The characteristics of the signal strength is highly dependent on the local night and day.

The Sun's energy ionizes the Earth's atmosphere during the day. This produces different ionization layers defined as layers D, E, F. At night, there is only ionization from cosmic waves, and therefore there is only an F layer (1).

VLF radio waves reflect off the free electrons in the different ionosphere layers. The signal strength of this reflected signal can be detected by a SID small radio telescope. The normal use of the SID radio telescope is to detect solar flares which appear as short term signal strength increases during the daytime monitoring. The author will use the SID telescope's capability to measure and analyze the VLF signal strength variations and the effect of the solar eclipse on the ionosphere.

The total solar eclipse on August 21, 2017 in North America provides an opportunity to analyze the differences between the eclipse and normal daily ionospheric reflections.

## 1.2 Past Eclipse History

The 1999 total solar eclipse which traced its umbra through Europe was documented with multiple radio telescopes. (2) The lead investigator for this effort, Dr. Bamford, recorded a 1440 kHz signal increase during this eclipse. (figure 2)

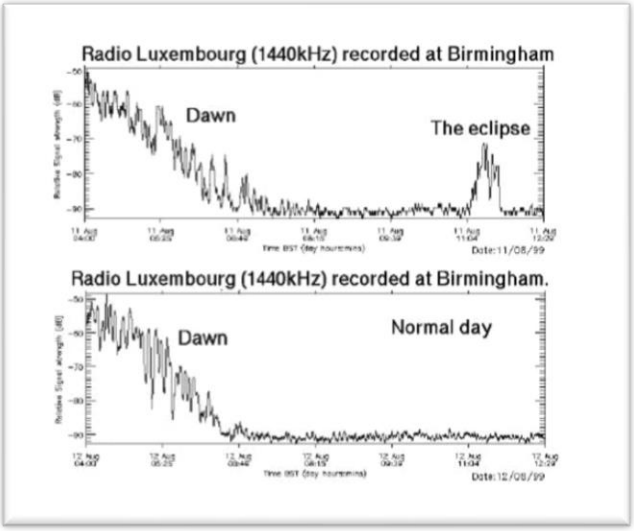


*Figure 1: 1440 kHz Signal Variation for 1999 Eclipse (2)*

This eclipse signature indicates that at 1440 kHz, that there is enough change in reflection of the ionosphere to cause a noticeable spike in signal. This increase in signal is similar to the effects of a solar flare on the signal levels of the SID radio telescope. This led to the question if the SID telescope can detect the eclipse and what would the signal look like?

The author has been using the SID radio telescope for over a year as an official observer for AAVSO. By chance, the eclipse umbra is passing between the VLF transmitter station and the author's SID radio telescope. This provides a unique opportunity to compare over a year's historic data with the eclipse data. In order to gain insight into the possible effects of the eclipse, the author developed two predictive models using historic data and eclipse times.

The following analysis develops these models to predict the signal levels during the 2017 eclipse.

## 1.1 Approach

The goal of this analysis is to predict the variations caused by the eclipse by analyzing the past signal strength slope of the day and night transitions. The hypothesis of this report is that the rate of the signal strength increases is fast enough to cause a detectable signal on the SID radio telescope data.

The slopes of the night-to-day and the day-to-night signals for a year of SID data were measured as part of the American Association of Variable Star Observers (AAVSO) (3). The slope rates were applied to the predicted time the eclipse will intersect the line between the VLF station in North Dakota [i]and the SID receiving station in Colorado.

The difference between the predicted signal characteristics and the data from the actual eclipse may allow for a unique insight into the short-term variation of the ionosphere during an eclipse.

## 2.0 SuperSID Monitor Measurements

The measurements were conducted using a SuperSID receiver and antenna (figure 2) procured by Stanford (4) Measurements were made in support of the AAVSO (3) observer program. A full year of measurements were analyzed.


*Figure 2: Colorado Springs SuperSID Monitoring Station*

## 2.1 Transmitter Stations

The VLF station used for this analysis was the LaMoore, North Dakota station located at Latitude 46.35N and Longitude -98.33W broadcasting at 25.2 kHz and 500 kWatts. The receiving station is located in Colorado Springs, Colorado. Figure 3 shows the other available VLF stations used by the SID measurement program (1). The LaMoore station has provided the author the most reliable measurements since the telescope was set up.

***Appendix A - VLF Station List[10]***

See http://sidstation.lionelloudet.homedns.org/stations-list-en.xhtml for a current version of this list.

| *Country* | *Location* | *Name* | *Frequency* | *Power (kHz)* | *Latititude / Longitude* |
|---|---|---|---|---|---|
| **USA** | Cutler, ME | NAA | 24.0 | 1000 | 44.65 N -67.3 W |
| | Jim Creek, WA | NLK | 24.8 | 250 | 48.20 N -121.92 W |
| | Lualualei, HI | NPM | 21.4 | 566 | 20.4 N -158.2 W |
| | LaMoure, ND | NML | 25.2 | 500 | 46.35 N -98.33 W |
| | Aquada, Puerto Rico | NAU | 40.75 | 100 | 18.40 N -67.18 W |
| **Antarctica**: | South Pole | VLF | 20.0 | | -09 / 0 |
| **Australia** | Harold E. Holt (North West Cape) | NWC | 19.8 | 1000 | -21.8 114.2 E |
| **China[11]:** | Changde | 3SA (alternates 3SB) | 20.6 | | 25.03 111.67 |
| | Datonge | 3SB (alternates 3SA) | 10.6 | | 35.60 103.33 |
| **France:** | Rosnay | HWU | 20.9 | 400 | 40.7N 1.25E |
| | St. Assie | FTA[12] | 16.8 | | |
| | LeBlanc (NATO) | HWV | 21.75 | | 40.7 N, 1.25 E |
| **Germany:** | Rhauderfehn | DHO | 23.4 | 500 | 53° 10' N 07° 33'E |
| **Iceland:** | Keflavik (US Navy) | NRK | 37.5 | 100 | 65N -18E |
| | Keflavic | TFK | 37.5 | | |
| **India:** | Katabomman | VTX3 | 18.2 | | 8.47 77.40 |
| **Italy:** | Tavolara | ICV | 20.27 | 43 | 40.88N 9.68E |
| | Sicily | NSC | 45.9 | | 38N 13.5E |
| **Japan:** | Ebino | JJI | 22.2 | | 32.04 130.81 |
| **Norway[13]:** | Kolsas | JXN | 16.4 | 45 | 59.51N 10.52E |
| **Russia[14]:** | Arkhangelsk | UGE | 19.7 | 150 input | 64N24 41E32 |
| | Batumi | UVA | 14.6 | 100 input | |
| | Kaliningrad | UGKZ | 30.3 | 100 input | |
| | Matotchkinchar | UFQE | 18.1 | 100 input | |
| | Vladivostok | UIK | 15.0 | 100 input | |
| **Turkey** | Bafa | TBB | 26.7 | | 37.43 27.55 |
| **United Kingdom** | Anthorn | GBZ | 19.6 | 500 | 52:71N -3:07W |
| | Anthorn (NATO) | GQD | 22.1 | 500 | 52:4N -1.2W |
| | London | GYA | 21.37 | 120 | 51 N 2 E |

There is no transmitter below 18.3 kHz usable for SID monitoring in Europe.

*Figure 3: VLF Station List (1)*

## 2.3 Measurement and Analysis Process

An example daily output of the SID monitor is shown in figure 4.

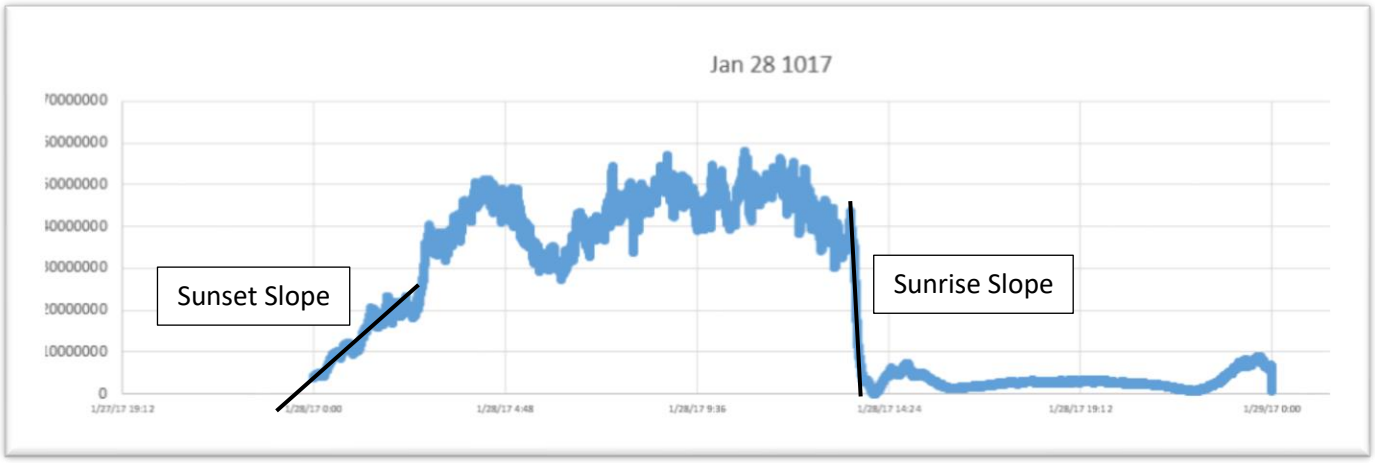


*Figure 4: SID Monitor Output for January 28, 2017*

At sunset, the signal strength increases and is variable throughout the night. Near sunrise the signal strength drops rapidly. There is normally a characteristic bump just after sunrise and again before sunset. The signal also has a slight curve during the middle of the day. The lines for sunset and sunrise shows where the slopes will be measured for the historic models.

The SID data for the past year was transferred from the SID software format to Microsoft Excel. The data was plotted for each day and the sunset and sunrise slopes were measured.

## 2.4 Sunset and Sunrise Rate Analysis

The initial methodology was to analyze every daily plot for the entire year and then determine if there was a trend or pattern that could be used to predict the August 21, 2017 conditions. Daily slope data was tabulated for each day of January 2017 as shown in figure 5 for sunrise data and figure 6 for sunset data.

| Parameter | Value | | Date | Transmitter Sunrise | Receiver Sunrise | Start Time | Stop Time | Delta Time | Start Level | Stop Level | Delta Level | Rate per second |
|---|---|---|---|---|---|---|---|---|---|---|---|---|
| Sunrise Rate Mean | (15,742) | | 1-Jan-17 | | 14:09 | 13:38 | 14:09 | 1860 | 19,744,646 | 1,352,493 | (18,392,153) | (9,888) |
| Sunrise Rate Stdev | 5,493 | -34.9% | 2-Jan-17 | | | 13:38 | 13:58 | 1200 | 14,838,240 | 1,786,398 | (13,051,842) | (10,877) |
| Sunset Rate Mean | | | 3-Jan-17 | | | 13:46 | 14:10 | 1440 | 13,057,672 | 64,983 | (12,992,689) | (9,023) |
| Sunset Rate StDev | | | 4-Jan-17 | | | 13:38 | 14:03 | 1500 | 24,122,396 | 108,927 | (24,013,470) | (16,009) |
| | | | 5-Jan-17 | | | 13:43 | 14:04 | 1260 | 17,580,790 | 498,343 | (17,082,448) | (13,557) |
| | | | 6-Jan-17 | | | 13:38 | 14:04 | 1320 | 30,604,060 | 660,059 | (29,944,001) | (22,685) |
| | | | 7-Jan-17 | | | 13:39 | 14:04 | 1500 | 32,045,405 | 1,599,783 | (30,445,622) | (20,297) |
| | | | 8-Jan-17 | | | 13:32 | 14:02 | 1800 | 37,381,881 | 1,194,586 | (36,187,296) | (20,104) |
| | | | 9-Jan-17 | | | 13:28 | 14:00 | 1920 | 39,712,508 | 2,317,404 | (37,395,104) | (19,477) |
| | | | 10-Jan-17 | | | 13:15 | 14:06 | 3060 | 40,254,206 | 721,819 | (39,532,387) | (12,919) |

*Figure 5: Sunrise Rate Analysis Data – January 2017*

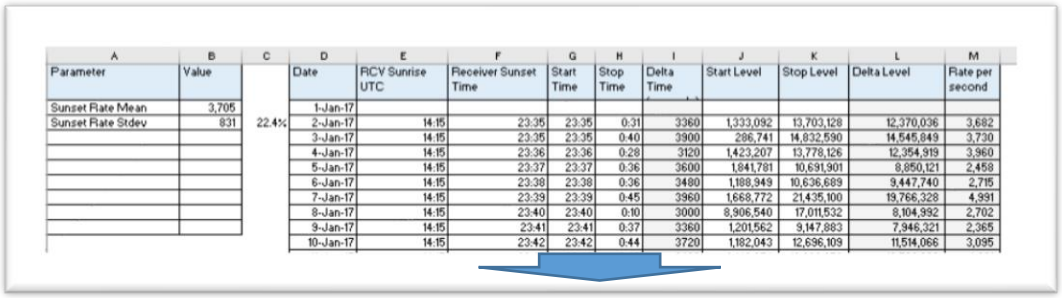

| Parameter | Value | | Date | RCV Sunrise UTC | Receiver Sunset Time | Start Time | Stop Time | Delta Time | Start Level | Stop Level | Delta Level | Rate per second |
|---|---|---|---|---|---|---|---|---|---|---|---|---|
| Sunset Rate Mean | 3,705 | | 1-Jan-17 | | | | | | | | | |
| Sunset Rate Stdev | 831 | 22.4% | 2-Jan-17 | 14:15 | 23:35 | 23:35 | 0:31 | 3360 | 1,333,092 | 13,703,128 | 12,370,036 | 3,682 |
| | | | 3-Jan-17 | 14:15 | 23:35 | 23:35 | 0:40 | 3900 | 286,741 | 14,832,590 | 14,545,849 | 3,730 |
| | | | 4-Jan-17 | 14:15 | 23:36 | 23:36 | 0:28 | 3120 | 1,423,207 | 13,778,126 | 12,354,919 | 3,960 |
| | | | 5-Jan-17 | 14:15 | 23:37 | 23:37 | 0:36 | 3600 | 1,841,781 | 10,691,901 | 8,850,121 | 2,458 |
| | | | 6-Jan-17 | 14:15 | 23:38 | 23:38 | 0:36 | 3480 | 1,188,949 | 10,636,689 | 9,447,740 | 2,715 |
| | | | 7-Jan-17 | 14:15 | 23:39 | 23:39 | 0:45 | 3960 | 1,668,772 | 21,435,100 | 19,766,328 | 4,991 |
| | | | 8-Jan-17 | 14:15 | 23:40 | 23:40 | 0:10 | 3000 | 8,906,540 | 17,011,532 | 8,104,992 | 2,702 |
| | | | 9-Jan-17 | 14:15 | 23:41 | 23:41 | 0:37 | 3360 | 1,201,562 | 9,147,883 | 7,946,321 | 2,365 |
| | | | 10-Jan-17 | 14:15 | 23:42 | 23:42 | 0:44 | 3720 | 1,182,043 | 12,696,109 | 11,514,066 | 3,095 |

*Figure 6: Sunset Rate Analysis - January 2017*

A control chart for the sunset and sunrise slopes was set up. The mean sunset and sunrise slope was calculated. The upper and lower control limits were set at 1 standard deviation above and below the mean. The January 2017 control chart is shown in figures 7 and 8.

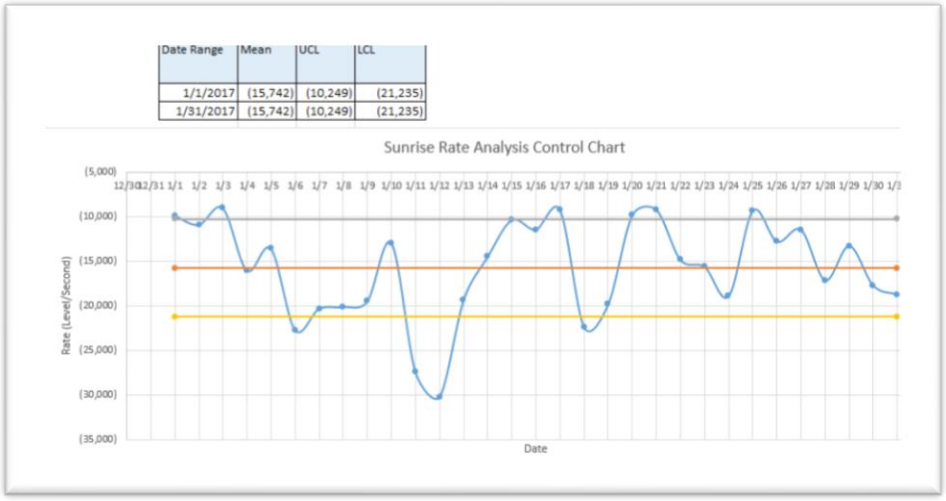


*Figure 7: January 2017 Sunrise Control Chart*


*Figure 8: January 2017 Sunset Control Chart*

The January 2017 control charts show that there is a cyclic variation in the both sunset and sunrise rates. The cause of these variations is unknown to the author and will be left for further research. Due to time requirements, a sample measurement was chosen for each month back to August 2016. The average rates for sunset and sunrise were calculated. (figure 9)

| SUNSET | |
|---|---|
| Date | Units/Second |
| 8/1/2016 | 11,972 |
| 9/2/2016 | 14,304 |
| 10/1/2016 | 9,472 |
| 11/1/2016 | 6,752 |
| 12/1/2016 | 3,701 |
| 1/1/2017 | 4,726 |
| 2/1/2017 | 4,449 |
| 3/1/2017 | 4,243 |
| 4/1/2017 | 2,327 |
| 5/1/2017 | 5,170 |
| Average | 6,712 |
| STDEV | 3,927 |

| SUNRISE | |
|---|---|
| Date | Units/Second |
| 8/1/2016 | (35,489) |
| 9/2/2016 | (71,812) |
| 10/1/2016 | (79,216) |
| 11/1/2016 | (20,391) |
| 12/1/2016 | (21,334) |
| 1/1/2017 | (11,529) |
| 2/1/2017 | (11,408) |
| 3/1/2017 | (32,054) |
| 4/1/2017 | (9,612) |
| 5/1/2017 | (17,727) |
| Average | (31,057) |
| STDEV | 24,976 |

*Figure 9: Monthly Rates for Sunrise and Sunset*

The rate data was plotted in figure 10. It was noted that the early data had higher magnitudes and variations in 2016. This could have been caused by measurement errors during the early SID radio telescope setup. The 2017 data appears to be more stable.

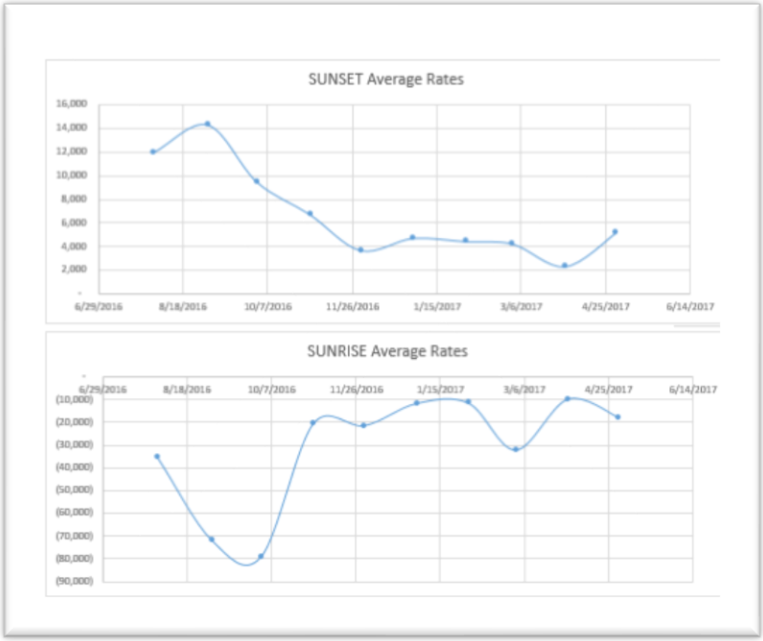


*Figure 10: Monthly SUNSET and SUNRISE Plots*

## 2.5 Yearly Measurement and Analysis

The data was plotted for each month over a year. (Figure 11). The goal of selecting given days was to get "clean" plots that did not have any solar flares or maintenance periods.

There is a change between the duration between sunset and sunrise over the year. This is indicative of the Earth's travel around the Sun.

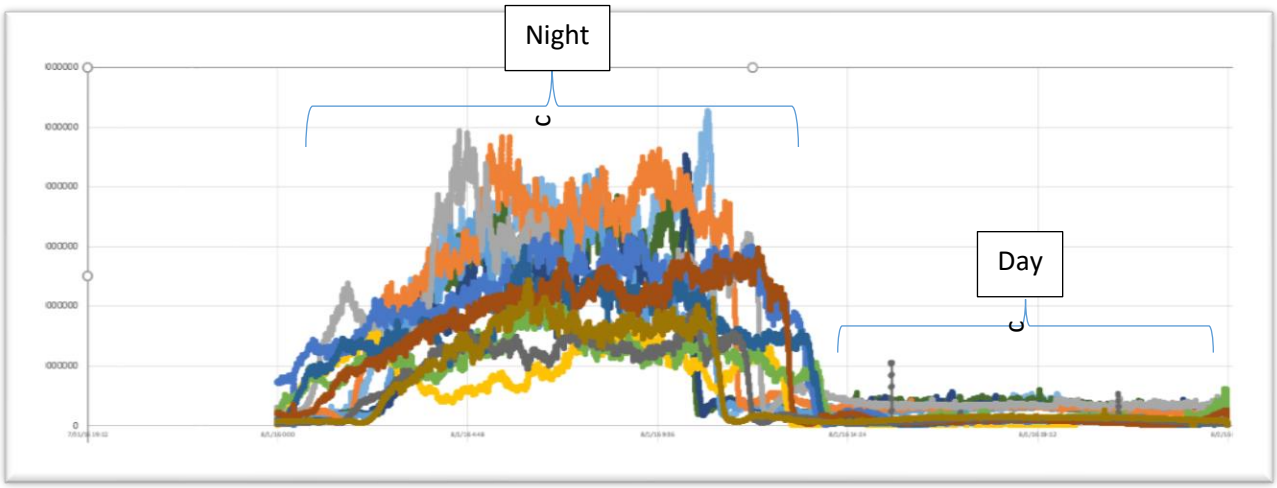


*Figure 11: Monthly Data Plots*

The rates appear to be dependent on time of year and the duration of the day. Radio Jupiter Pro (5) was used to calculate the sunrise and sunset times for the time period of the measurements. (figure 12) This data was used to validate that the sunrise and sunset rates can be related to night time duration.

| Date | Sunset | Sunrise | Night Duration | Sunset Rate | Sunrise Rate |
|---|---|---|---|---|---|
| 5/1/2016 | 1:38 | 12:03 | 10:25 | | |
| 6/1/2016 | 2:04 | 11:38 | 9:34 | | |
| 7/1/2016 | 2:15 | 11:38 | 9:23 | | |
| 8/1/2016 | 2:00 | 12:00 | 10:00 | 11972 | -35489 |
| 9/1/2016 | 1:22 | 12:26 | 11:04 | 14304 | -71812 |
| 10/1/2016 | 0:35 | 12:52 | 12:17 | 9472 | -79216 |
| 11/1/2016 | 23:52 | 13:22 | 13:30 | 6752 | -20391 |
| 12/1/2016 | 23:30 | 13:54 | 14:24 | 3701 | -21334 |
| 1/1/2017 | 23:38 | 14:15 | 14:37 | 4726 | -11529 |
| 2/1/2017 | 0:09 | 14:04 | 13:55 | 4449 | -11408 |
| 3/1/2017 | 0:40 | 13:32 | 12:52 | 4243 | -32054 |
| 4/1/2017 | 1:10 | 12:45 | 11:35 | 2327 | -9612 |
| 5/1/2017 | 1:38 | 12:03 | 10:25 | 5170 | -17727 |
| 6/1/2017 | 2:04 | 11:38 | 9:34 | | |
| 7/1/2017 | 2:15 | 11:38 | 9:23 | | |
| 8/1/2017 | 2:00 | 11:59 | 9:59 | | |
| 8/21/2017 | 1:37 | 12:16 | 10:39 | | |
| 9/1/2017 | 1:22 | 12:26 | 11:04 | | |

*Figure 12: Night Durations against Measured Sunset and Sunrise Rates*

The sunrise and sunset rates were plotted in figure13 to determine if there were any useable trends. The results indicate that there were no obvious trends that can be used to help in the August 21, 2017 prediction.

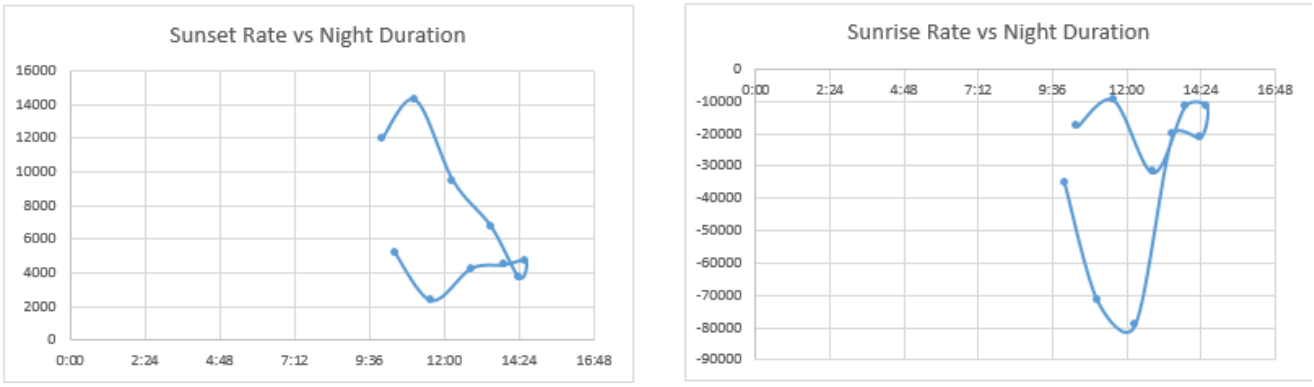


*Figure 13: Rates vs Night Duration*

The approach to estimating the August 21, 2017 profile shifted to mapping the August 2016 data. The first step was to validate if the yearly variations were representative. The May 2016 and May 2017 data was available to compare a full year difference. This data was plotted in figure 14.

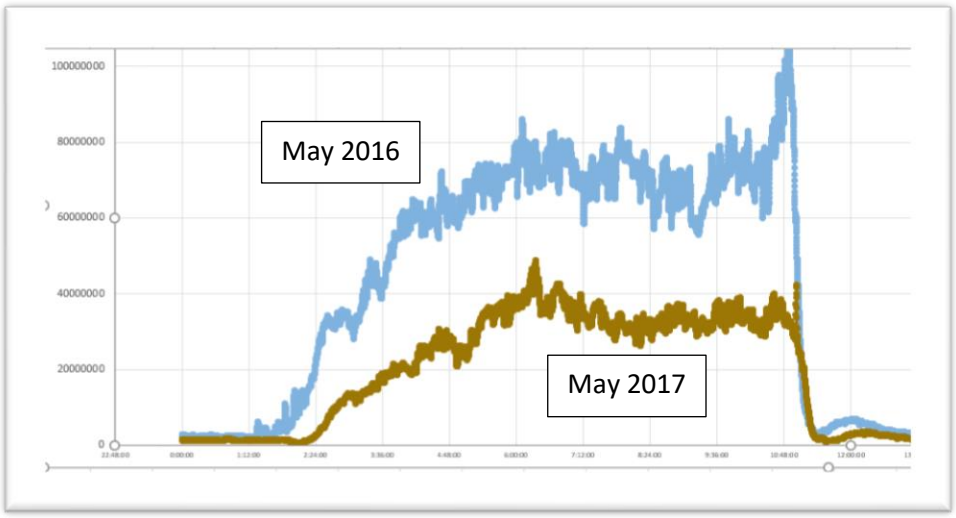


*Figure 14: May 2016 and May 2017 Plots*

Figure 14 shows that there is a variation in signal level and sunset start time and rate. However, the sunrise slope rate and time looks very close between the plots.

This bodes the question if the data can be related per month. The sunset start plots were compared in figure 15. Note: A SID operator noted that the plot of sunrise and sunset were symmetric on his plots. His station did not have any mountains. A theory is that the author's site is affected during sunset by the Pikes Peak mountain range to the west. The eclipse would not be affected by the mountains. The net symmetric slope increase would therefore result in a faster rise and higher signal level before totality.

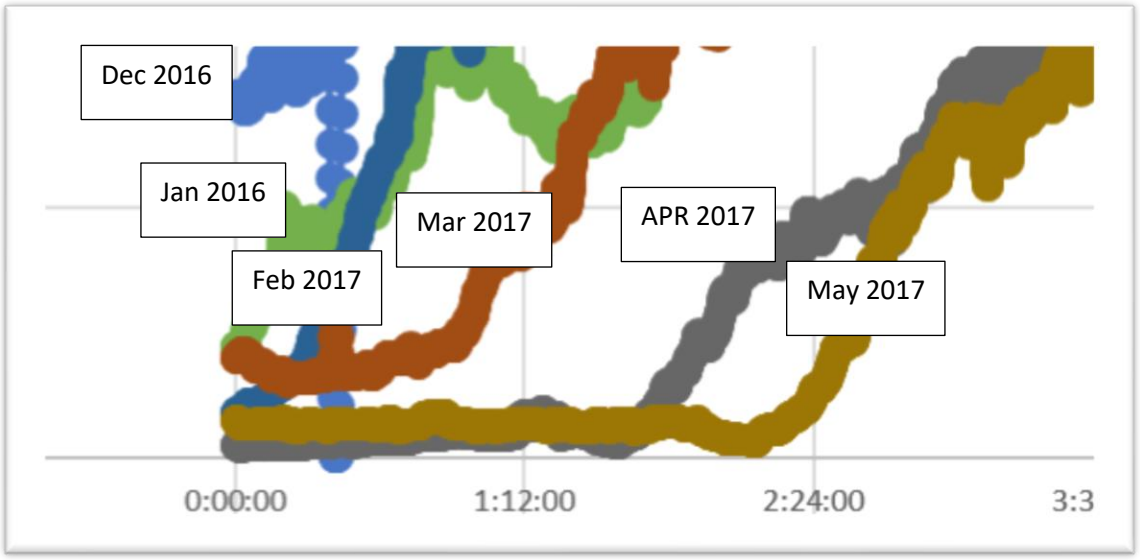


*Figure 15: Sunset Start Time Plots*

The sunset start time do correlate with the sunset times for each month. Note that the sunset start time and the signal increases move to the right from December to May. There does not appear to be a correlation with sunset slope rates based on month.

The sunrise plots were plotted in figure 16. The sunrise start times move to the left from December to May.

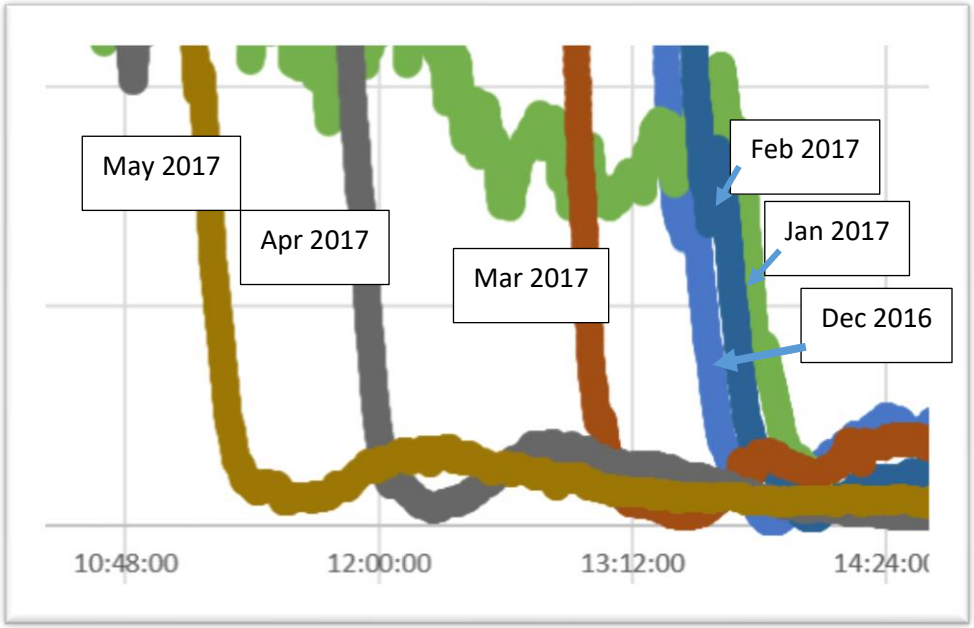


*Figure 16: Sunrise Plots*

The sunrise plots also show the March to April plots are spread out and the Dec 2016 to Feb 2017 plots are bunched up. The sunrise plots also indicate a more consistent slope rate for each month. This may indicate

that at sunrise the signal level drops dramatically possibly independent of the time of year. This is in contrast to the sunset rates that have a variation of the slope rate throughout the year.

## 3.0 Eclipse and VLF Signal Geometry

The solar eclipse forms when the Moon crosses between the Sun and the Earth. A total eclipse forms the umbra and a partial eclipse forms the penumbra. (figure 17)

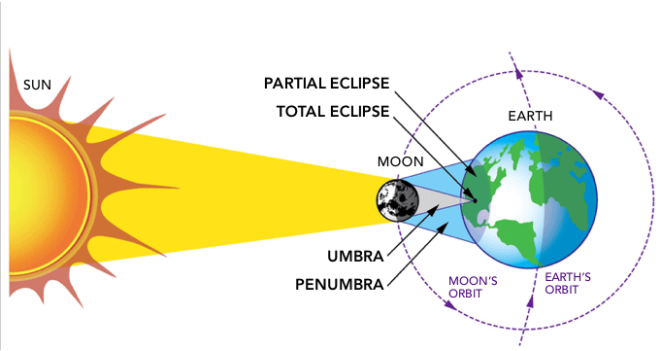


*Figure 17:Eclipse Basics (6)*

NASA has plotted the umbra and penumbra for the August 21 path through North America. The umbra and penumbra happens to cross through the line between the LaMoore, North Dakota VLF station and the author's SID radio telescope in Colorado Springs, Colorado. (figure 18)

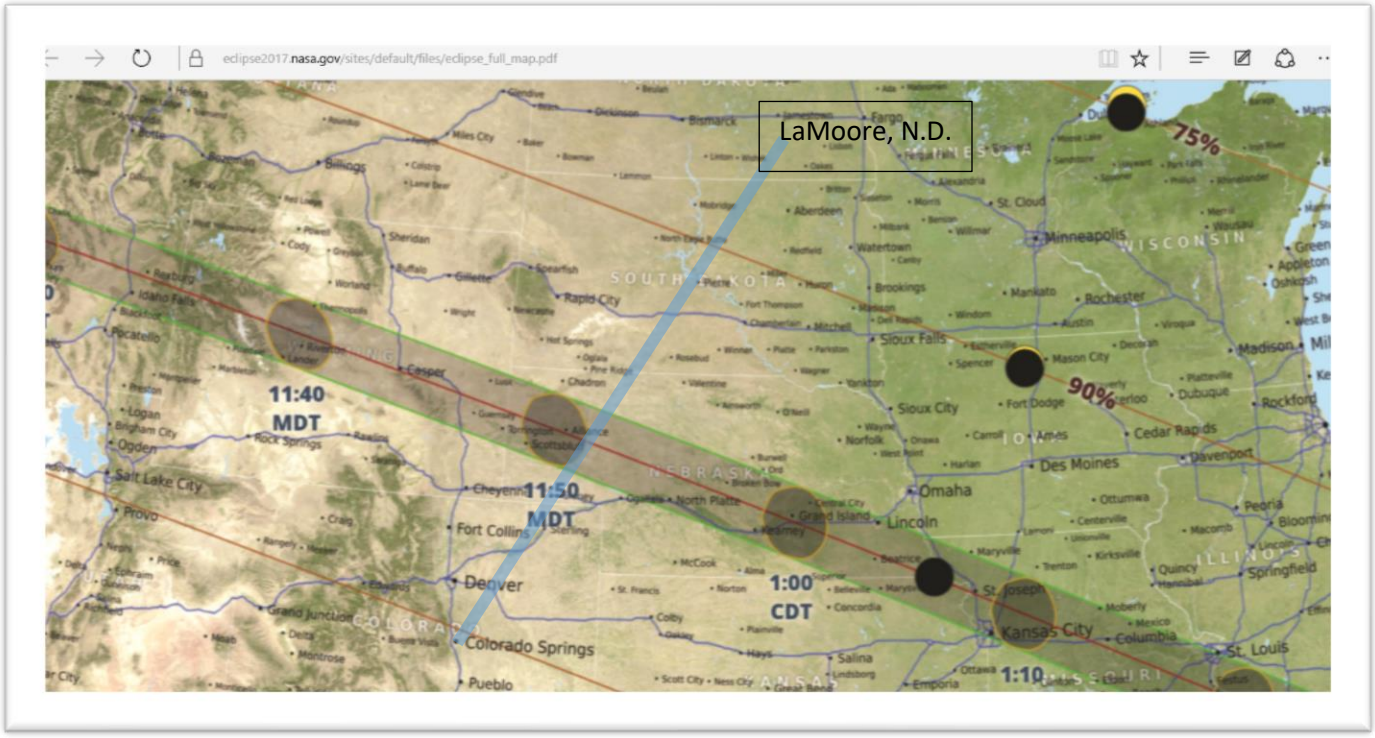


*Figure 18: Eclipse Path (7) (8)*

NASA also published the times for the eclipse for major cities along the path. (figure 19)

| | Eclipse Begins | Totality Begins | Totality Ends | Eclipse Ends | |
|---|---|---|---|---|---|
| *Madras, OR* | 09:06 a.m. | 10:19 a.m. | 10:21 a.m. | 11:41 a.m. | PDT |
| *Idaho Falls, ID* | 10:15 a.m. | 11:33 a.m. | 11:34 a.m. | 12:58 p.m. | MDT |
| *Casper, WY* | 10:22 a.m. | 11:42 a.m. | 11:45 a.m. | 01:09 p.m. | MDT |
| *Lincoln, NE* | 11:37 a.m. | 01:02 p.m. | 01:04 p.m. | 02:29 p.m. | CDT |

*Figure 19: Eclipse Schedule (9)*

One of the key predictions will be to determine when the start, totality and end of the eclipse will appear for the SID radio telescope. The VLF path line crosses the full totality point at the 11:50 AM point. Using the Casper, WY schedule in figure 18, the rough estimate is that the times should be adjusted by + 8 minutes. Add 6 hours to convert from Mountain Daylight time gives:

Eclipse Begins: 1630 UTC
Totality Begins: 1750 UTC
Totality Ends: 1753 UTC
Eclipse Ends: 1917 UTC

### 3.1 Calculating the Eclipse Area over Time

As the Moon passes in front of the Sun, it subscribes an arc *abc*. The total area eclipsed is therefore areas (A1+A2). (figure 20)

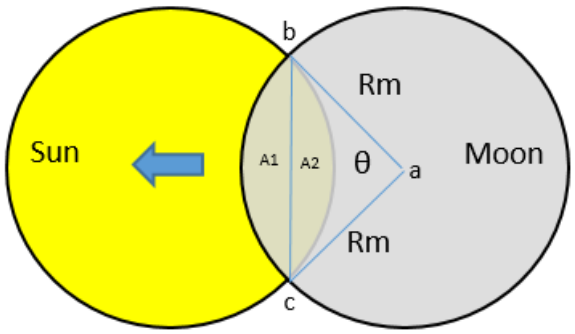


*Figure 20: Sun and Moon Eclipse Geometry*

For the eclipse, a close approximation can be made that the apparent diameter of the Sun and Moon are the same. The area of A1 is the area of arc segment abc with the triangle abc removed. The formulas for these are shown below.

$$Area\ Arc\ abc = \frac{\theta}{360}\pi r_m^2 \qquad (1)\ (10)$$

Area A1 = Area Arc abc – Area Δabc (2)

The geometry of triangle abc (Δabc) is shown in figure 21.

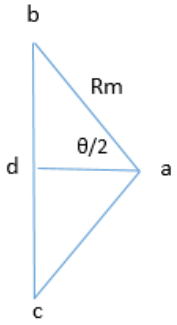


*Figure 21: Triangle abc Geometry*

Area Δabc = (2) Area Δabd (3)

Note that Δabc is an isosceles triangle with lines ab and ac being equal with central angle θ. By finding the line ad and line bd, the area of Δabd can be found. Note that Rm is the Apparent Moon radius.

Line ad = (Rm) cos(θ/2) (4)

Line bd = (Rm) sin((θ/2) (5)

The area of Δabc is therefore:

$$\text{Area } \Delta abc = (2)\text{Area } \Delta abd = (2)\frac{1}{2}(R_m^2)\cos\left(\frac{\theta}{2}\right)\sin\left(\frac{\theta}{2}\right) = (R_m^2)\cos\left(\frac{\theta}{2}\right)\sin\left(\frac{\theta}{2}\right) \quad (6)$$

Finally, the area of A1 is:

Area A1 = Area arc abc - Area Δabc (7)

Assume that the apparent radius of the Moon is the same as the apparent radius of the Sun for the eclipse. Therefore, the area A1 = A2. So, the total eclipse area can now be calculated as:

$$Total\ Eclipse\ Area = (2)Area\ A1 = (2)\left(\frac{\theta}{360}\pi r_m^2 - (\boldsymbol{R_m^2})\boldsymbol{cos}\left(\frac{\boldsymbol{\theta}}{\boldsymbol{2}}\right)\boldsymbol{sin}\left(\frac{\boldsymbol{\theta}}{\boldsymbol{2}}\right)\right) \quad (8)$$

$$Total\ Eclipse\ Area = r_m^2\left(\frac{\theta}{180}\pi - 2\boldsymbol{cos}\left(\frac{\boldsymbol{\theta}}{\boldsymbol{2}}\right)\boldsymbol{sin}\left(\frac{\boldsymbol{\theta}}{\boldsymbol{2}}\right)\right) \quad (9)$$

The analysis requires the calculation of the percent of the Sun that is eclipsed over time. Using the assumption that for the eclipse Rm = Rs (Sun's apparent radius):

$$Percent\ Sun\ Eclipsed = \frac{Total\ Eclipse\ Area}{Total\ Sun\ Area} = \frac{r_m^2\left(\frac{\theta}{180}\pi - 2\cos\left(\frac{\theta}{2}\right)\sin\left(\frac{\theta}{2}\right)\right)}{\pi r_s^2} \qquad (10)$$

With Rm = Rs

$$Percent\ Sun\ Eclipsed = \frac{\theta}{180} - \frac{2}{\pi}\cos\left(\frac{\theta}{2}\right)\sin\left(\frac{\theta}{2}\right) \qquad (11)$$

Equation 11 allows for the calculation of the percentage of the Sun that is being eclipsed without knowing the apparent radius of either the Sun or the Moon.

Now relate angle θ with time. The start and end of the eclipse θ =0°, while at totality θ = 180°.

The calculated results for the Sun eclipse area % for the entire eclipse period is shown if figure 22.

| Time | Delta Time (Min) | Theta (deg) | % Sun Eclipsed |
|---|---|---|---|
| 16:30 | 0 | 0.0 | 0.0% |
| 16:38 | 8 | 18.0 | 0.2% |
| 16:47 | 17 | 36.0 | 1.3% |
| 16:55 | 25 | 54.0 | 4.2% |
| 17:03 | 33 | 72.0 | 9.7% |
| 17:12 | 42 | 90.0 | 18.2% |
| 17:20 | 50 | 108.0 | 29.7% |
| 17:28 | 58 | 126.0 | 44.2% |
| 17:37 | 67 | 144.0 | 61.3% |
| 17:45 | 75 | 162.0 | 80.2% |
| 17:54 | 84 | 180.0 | 100.0% |
| 18:02 | 92 | 162.0 | 80.2% |
| 18:10 | 100 | 144.0 | 61.3% |
| 18:19 | 109 | 126.0 | 44.2% |
| 18:27 | 117 | 108.0 | 29.7% |
| 18:35 | 125 | 90.0 | 18.2% |
| 18:44 | 134 | 72.0 | 9.7% |
| 18:52 | 142 | 54.0 | 4.2% |
| 19:00 | 150 | 36.0 | 1.3% |
| 19:09 | 159 | 18.0 | 0.2% |
| 19:17 | 167 | 0.0 | 0.0% |

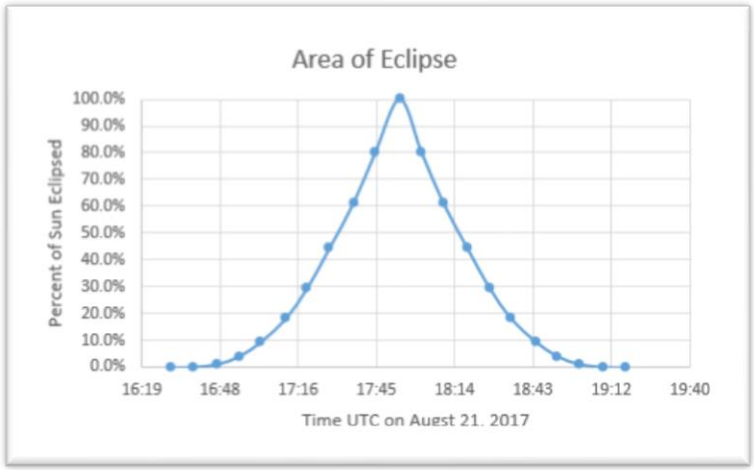


*Figure 22: Calculations and Plot for % Sun Eclipsed over Time (Corrected)*

## 5.0 Eclipse Models

Two models were developed to estimate the eclipse signal levels. (1) Historic data mapping and (2) Rate analysis

### 5.1 Historic Data Mapping

The data from Mar 1, 2017 was chosen as a template because of the smoothness of the signal for both sunset and sunrise rates. The approach was to connect the sunset data to the eclipse start time and meet the sunrise data which was started from the eclipse end time. (figure 23)

The characteristic of this model shows that the ionization layer builds up fast and results in a quick drop of signal level.

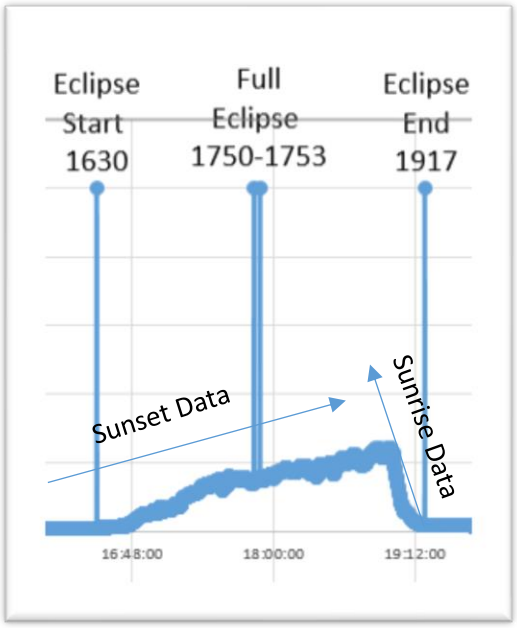


*Figure 23: Historic Model*

### 5.2 Rate Analysis using the Percent of Sun Area Eclipsed

The rates for sunset and sunrise were applied to the time and percentage of Sun being eclipsed. There are two parts to the model. The start of the eclipse to totality and then the totality to end of the eclipse.

The model on the start of the eclipse uses the sunset rate x the percent of Sun eclipsed. This is added incrementally until totality. This model emulates a normal sunset with the exception that the transit speed of the Moon is different than sunset and that the umbra area is smaller than a total nightfall.

The second half of the model starts with totality. This part of the model still uses the sunset rate and percentage of the Sun eclipsed. It then adds the sunrise rates x the percentage of the Sun not eclipsed. This simulates a sunrise with the exception that the Moon uncovers the area of the Sun shining at a different rate.

The results of this calculation and plot is shown on figure 24.

| Time | Delta Time (Min) | Theta (deg) | % Sun Eclipsed | Rate Analysis (Units) |
|---|---|---|---|---|
| 16:30 | 0 | 0.0 | 0.0% | 799,905 |
| 16:38 | 8 | 18.0 | 0.2% | 805,178 |
| 16:47 | 17 | 36.0 | 1.3% | 851,939 |
| 16:55 | 25 | 54.0 | 4.2% | 988,797 |
| 17:03 | 33 | 72.0 | 9.7% | 1,302,155 |
| 17:12 | 42 | 90.0 | 18.2% | 1,960,647 |
| 17:20 | 50 | 108.0 | 29.7% | 2,918,317 |
| 17:28 | 58 | 126.0 | 44.2% | 4,343,799 |
| 17:37 | 67 | 144.0 | 61.3% | 6,565,112 |
| 17:45 | 75 | 162.0 | 80.2% | 9,147,633 |
| 17:54 | 84 | 180.0 | 100.0% | 12,771,887 |
| 18:02 | 92 | 162.0 | 80.2% | 12,397,322 |
| 18:10 | 100 | 144.0 | 61.3% | 8,601,185 |
| 18:19 | 109 | 126.0 | 44.2% | 854,789 |
| 18:27 | 117 | 108.0 | 29.7% | (8,663,455) |
| 18:35 | 125 | 90.0 | 18.2% | (20,277,034) |
| 18:44 | 134 | 72.0 | 9.7% | (33,421,077) |
| 18:52 | 142 | 54.0 | 4.2% | (47,558,362) |
| 19:00 | 150 | 36.0 | 1.3% | (62,231,897) |
| 19:09 | 159 | 18.0 | 0.2% | (77,109,662) |
| 19:17 | 167 | 0.0 | 0.0% | (92,017,100) |

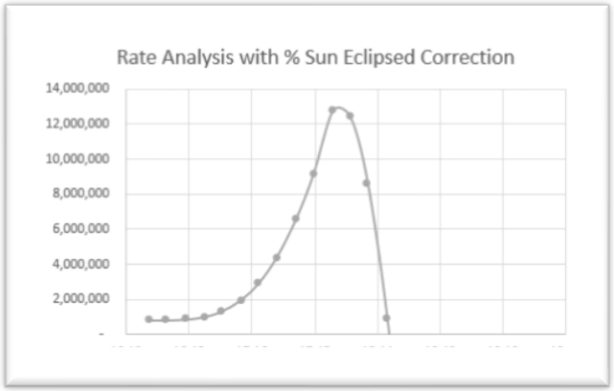


*Figure 24: Rate Data Corrected with Sun Area (Corrected)*

### 5.3 Combined Models

Combining the models against a daily plot shows two predicted results. (figure 25)

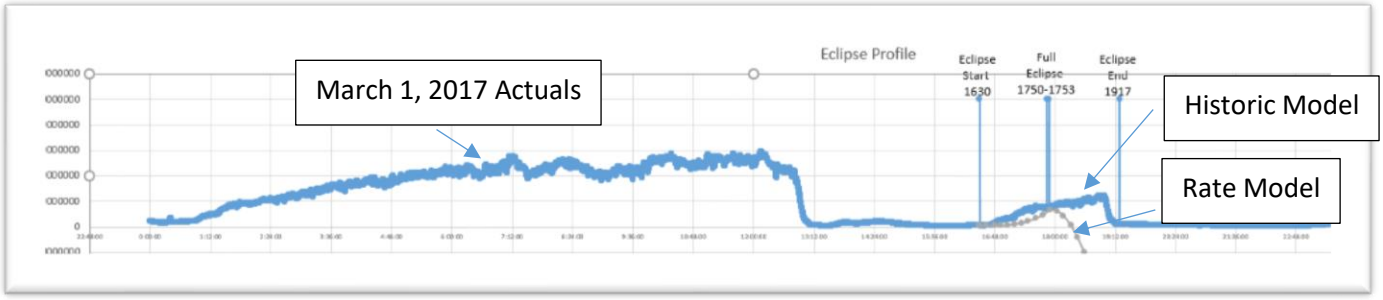


*Figure 25:Eclipse Models (Corrected)*

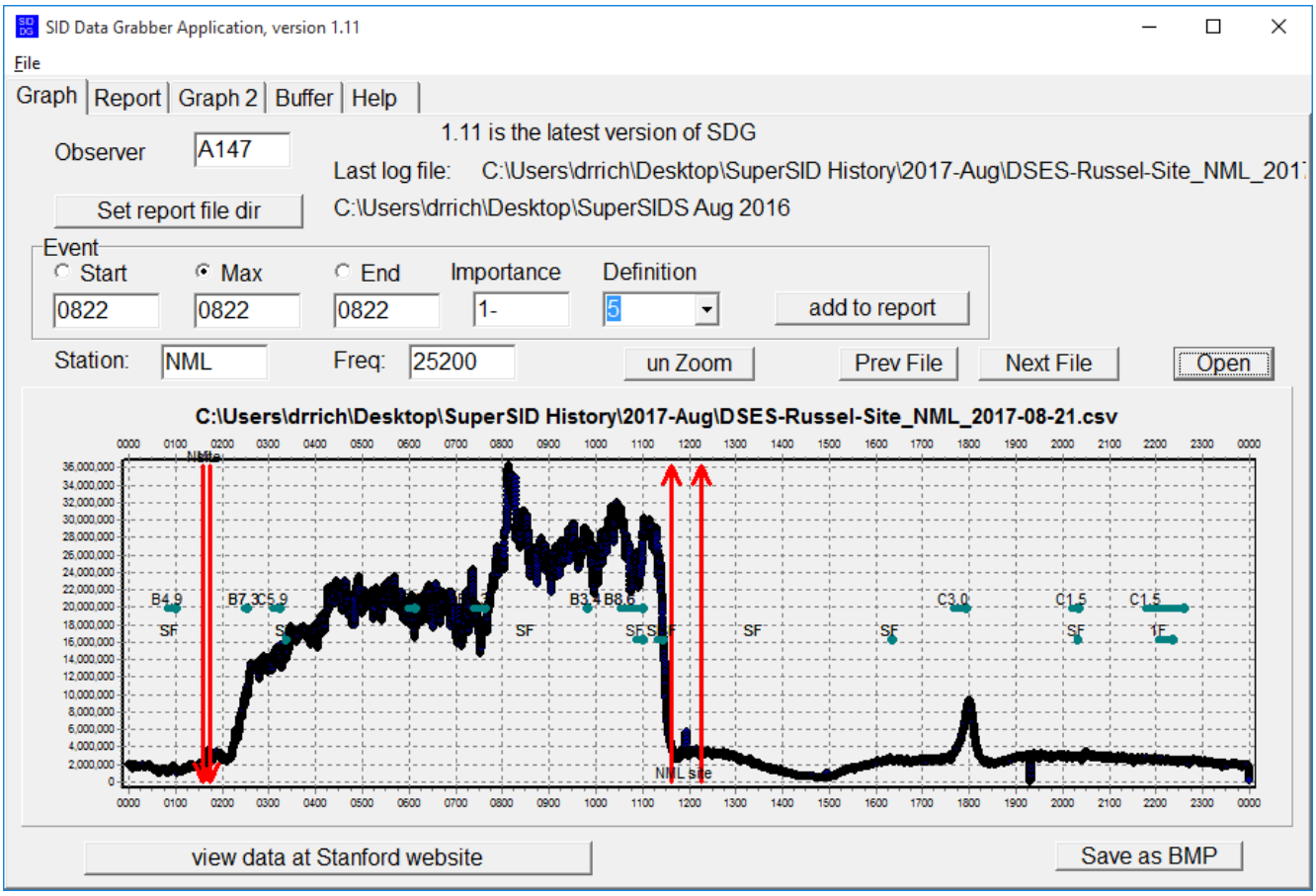
SID Data Grabber Application, version 1.11
File
Graph
Report
Graph 2
Buffer
Help
Observer
A147
1.11 is the latest version of SDG
Last log file: C:\Users\drrich\Desktop\SuperSID History\2017-Aug\DSES-Russel-Site_NML_201
Set report file dir
C:\Users\drrich\Desktop\SuperSIDS Aug 2016
Event
Start
Max
End
Importance
Definition
0822
0822
0822
1-
5
add to report
Station:
NML
Freq:
25200
un Zoom
Prev File
Next File
Open
C:\Users\drrich\Desktop\SuperSID History\2017-Aug\DSES-Russel-Site_NML_2017-08-21.csv
NML site
view data at Stanford website
Save as BMP

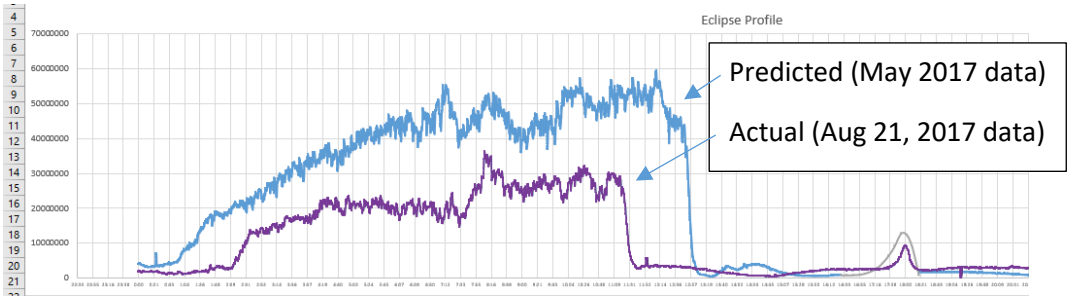
Eclipse Profile
Predicted (May 2017 data)
Actual (Aug 21, 2017 data)

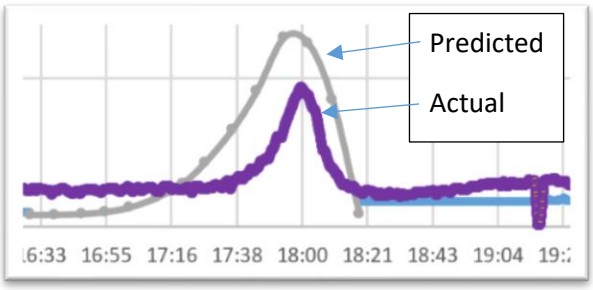
Predicted
Actual
16:55
17:16
17:38
18:00
18:21
18:43
19:04

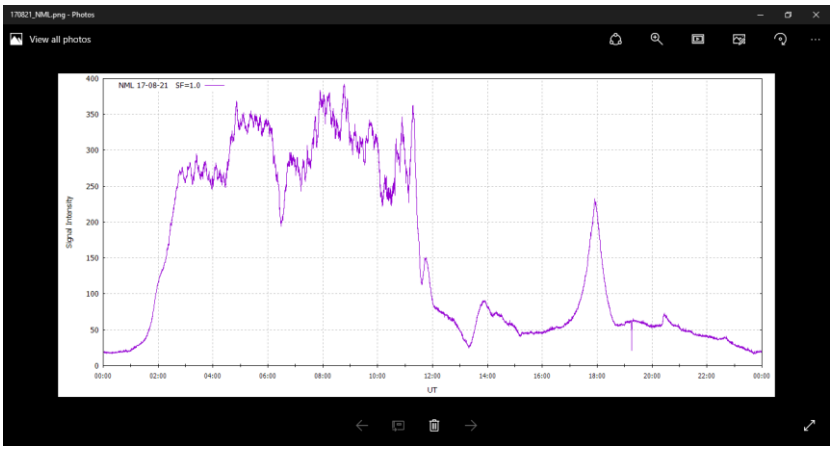


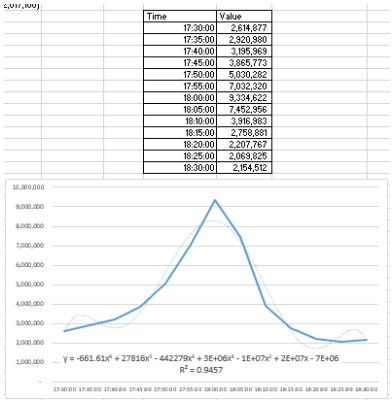

| Time | Value |
|---|---|
| 17:30:00 | 2,614,877 |
| 17:35:00 | 2,920,980 |
| 17:40:00 | 3,195,969 |
| 17:45:00 | 3,865,773 |
| 17:50:00 | 5,030,282 |
| 17:55:00 | 7,032,320 |
| 18:00:00 | 9,334,622 |
| 18:05:00 | 7,452,956 |
| 18:10:00 | 3,916,983 |
| 18:15:00 | 2,758,881 |
| 18:20:00 | 2,207,767 |
| 18:25:00 | 2,069,825 |
| 18:30:00 | 2,154,512 |



Correct for time

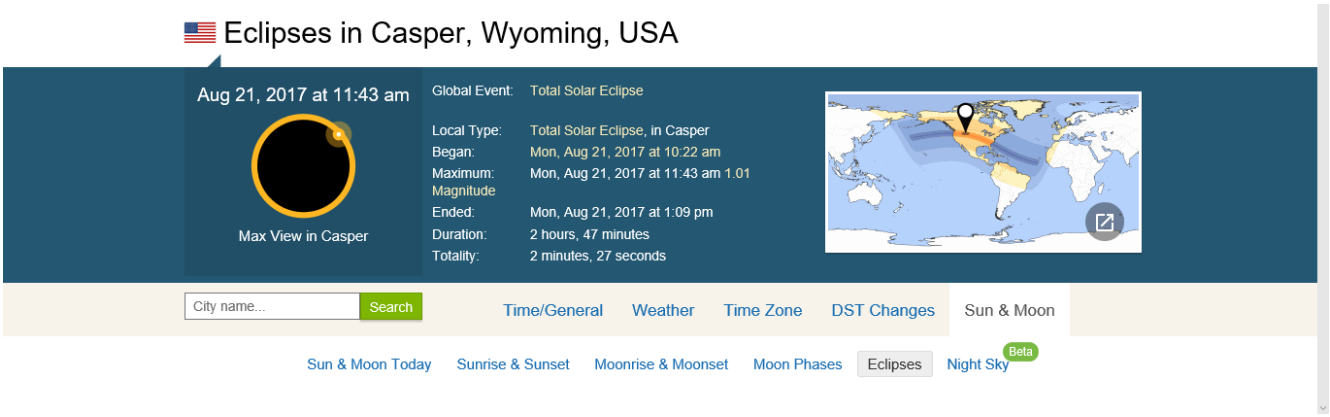


Start 10:23Local, Max: 11:48Local End:

Two fixes to the predicted model.

1) Update start and stop times for eclipse

2) Use August 21, 2017 sunset and sunrise rates in analysis

Adjusted for time

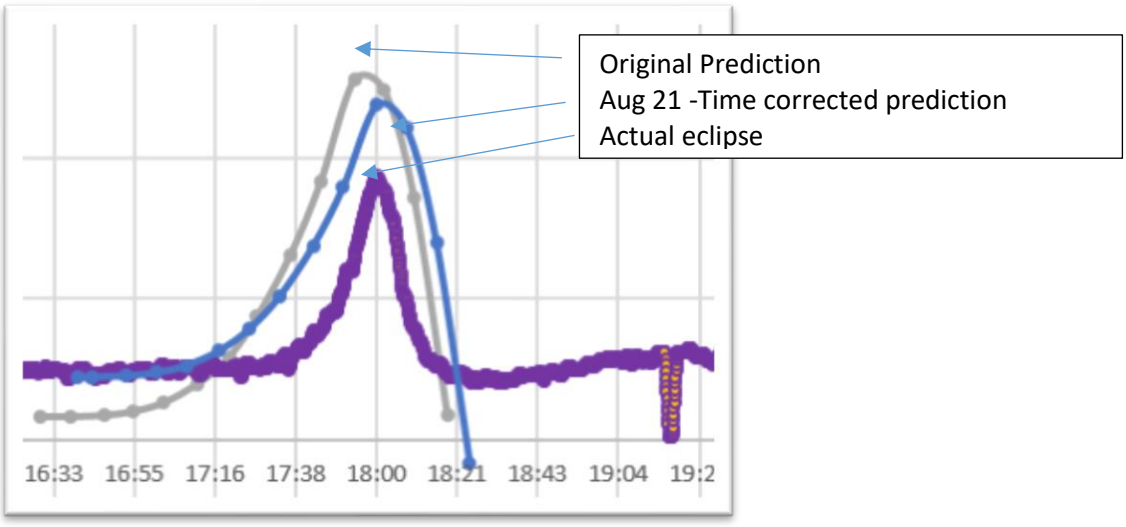


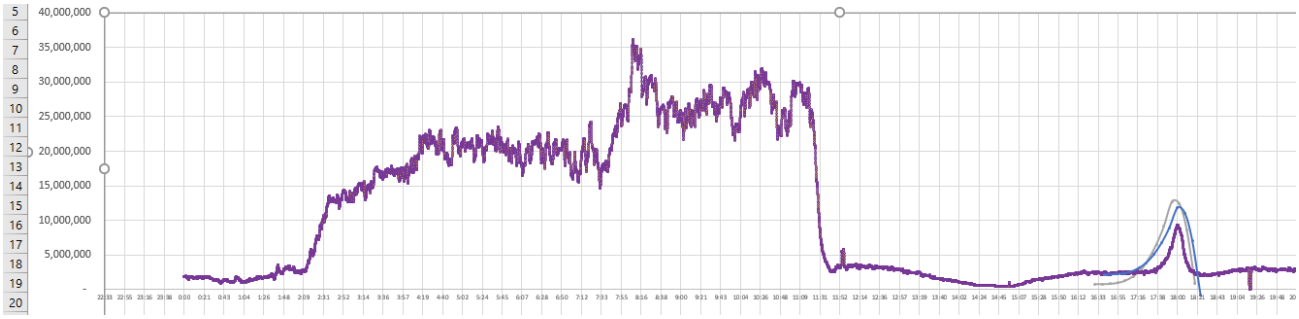


A zoom in on the eclipse period is shown on figure 26.

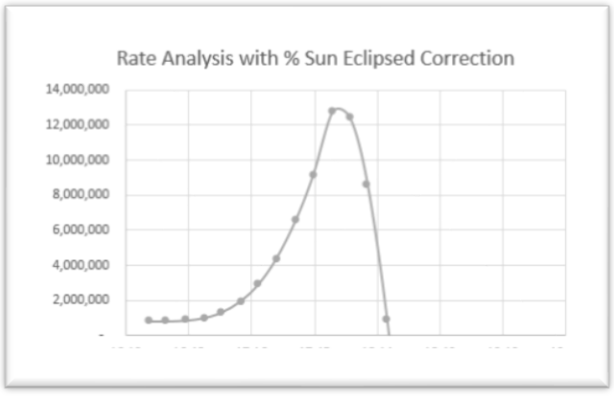


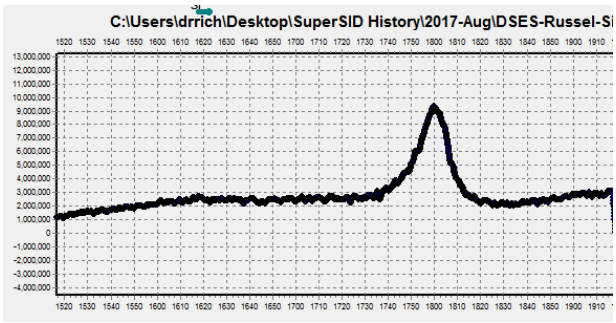

*Figure 26: Model Detail (Corrected)*

### 5.3 Analysis

Both models track together until the full eclipse. The historic model maintains a steady rise and then drops quickly to normal levels at eclipse end. This emulated a normal sunset and sunrise effect normalized to the time period of the eclipse.

The rate model uses historic rates and calculated Sun eclipse area over time to predict the signal strength. This model indicates that the Sun would quickly ionize the ionosphere and drop back to normal daytime levels before the end of the eclipse.

## 6.0 Theory of ionospheric reflection and refraction

$$Index\ of\ Refraction = \frac{c}{v_\phi} = \sqrt{1 - \frac{Nq^2}{\varpi^2 \epsilon m}}$$

C: speed of light

$v_Ø$: phase velocity

N: electron density (electrons/$cm^3$)

q: charge of electron (1.60 x 10-19 coulombs)

ε: dielectric constant (ε0=8.855 x 10-12 farad/m in free space)

m: mass of electron (9.11 x 10-31 kg)

$$critical\ frequency = 9.0\sqrt{N}$$

For 25.2 KHz (LaMoore, ND) the electron density required to reflect the signal is:

$$f = 9.0\sqrt{N}$$

$$N = (f/9.0)^2$$

$$N = (25{,}200/9.0)^2 = 7.84\ x10^6 \frac{electrons}{m^3} x \left(\frac{m}{100cm}\right)^3 = 7.84 \frac{electrons}{cm^3}$$

The NOAA Ionospheric electron density is:

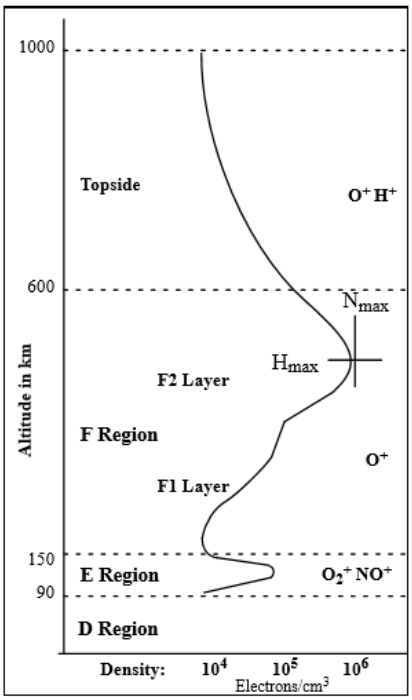


*Figure 27: Electron Density in the Ionosphere (11)*

Based on the electron density plot in figure 27, the 25.2 khz signal from LaMoore, ND is reflective in the E region and above. Therefore, the height of the D-Layer above the surface becomes the primary variable to model the signal path between two points on Earth.

### 6.1 Model to determine path length between two points on Earth

The calculation to determine the path length between two points on Earth.

$$d = R\sqrt{2 - 2cos\theta_1 cos\theta_2 \cos(\phi_1 - \phi_2) - 2sin\theta_1 sin\theta_2}$$

$$\alpha = sin^{-1}\left(\frac{d}{2R^2}\sqrt{4R^2 - d^2})\right)$$

$$\mathrm{D} = \mathrm{R}\alpha$$

Distance between LaMoure, ND (Latitude: 46.35N, Longitude: 98.33W) and Colorado Springs, CO receiver (Latitude: 38.85N, Longitude: 104.73W), R=6378 km

D= 984 km

Verified using calculator at: (12)

The radio wave will travel along the Earth-Ionosphere waveguide (12).

### 6.2 Find the reflection height above the surface

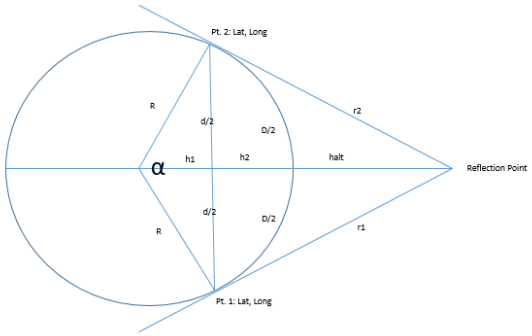


*Figure 28: Reflection Altitude geometry*

h1+h2 = R

h2= Rcos(α/2)

h1= R-h2 = R-Rcos(α/2)=R(1- cos(α/2))

Assume for reflection the reflection point angle = 90°

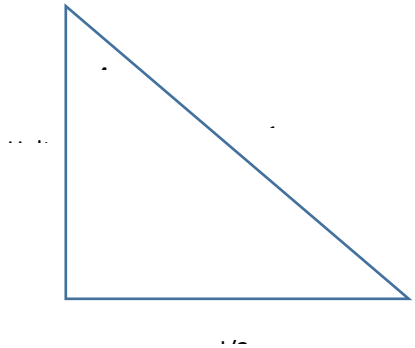

**d/2 = r1 sin(45°)**

**r1=d/(2 sin(45°))**

**halt+h1 = r1 sin(45°)**

**halt+h1=d/(2 sin(45°))**

## 7.0 Propagation of Radio Signals

## 7.0 Summary

The 2017 American solar eclipse provides a unique opportunity to observe the Sun's effect on the ionosphere using the SID radio telescope. The umbra of the eclipse will pass through the line from the

VLF transmission station and the receiving station. Data has been taken for over a year at the receiving station and was used to develop this baseline historic data.

The historic and rate analysis models provide a theoretical baseline into the understanding of the eclipse effects on the ionosphere. The tools and calculations developed to make these predictive models will help improve the data gathering and scientific experiment setup during the actual eclipse.

Data will be taken during the eclipse and compared to the predictive models. Variations between the actual versus predictive models may help in the understanding of the local Sun effects on the ionosphere and how quickly the ionosphere recovers to a normal daytime state.

## References


1. **Stanford Solar .** *SuperSID Manual: Space Weather Monitors.* s.l. : Stanford Solar Center, Stanford University, 2009.

2. **Bamford, Ruth.** *Radio and the 1999 UK Total Solar Eclipse.* Radio Communications Agency. Chilton, UK : s.n., 2000.

3. **American Association of Variable Star Observers. [Online] https://www.aavso.org/.**

**4.** ***SuperSID Manual - Space Weather Monitors.*** **Stanford University. Stanford, California : Stanford Solar Center.**

**5. Sky, Jim. radiosky.com. [Online] Radio Sky Publishing.**

**6. NASA. https://eclipse2017.nasa.gov/eclipse-who-what-where-when-and-ho. [Online]**

**7. https://eclipse2017.nasa.gov/sites/default/files/eclipse_full_map.pdf. [Online]**

**8. NASA. https://eclipse2017.nasa.gov/sites/default/files/eclipse_full_map.pd. [Online]**

**9. —. https://eclipse2017.nasa.gov/eclipse-who-what-where-when-and-. [Online]**

**10. Kohn, Ed.** ***CliffsQuickReview: Geometry.*** **s.l. : Wilet Publishing Inc, 2001. ISBN 0-7645-6380-7.**

**11. Pal, Sujay.** ***Numerical Modelling of VLF Radio Wave Propagation through Earth-Ionosphere Waveguide and its application to Sudden Ionospheric Disturbances.*** **University of Calcutta. Kolkata, India : s.n., 2013. Ph.D. Dissertation.**

**12.** ***Radio emission from cosmic ray air showers Monte Carlo simulations.*** **T. Huege, H. Falcke. July 26, 2013, Astronomy & Astrophysics.**

**13.** ***Atmospheric Ozone A Meteorological Factor in Low-Frequency and 160-meter Propagation.*** **Brown, Robert R. 2, Communications Quarterly Spring 1999, Vol. 9.**